



**CHALMERS**  
UNIVERSITY OF TECHNOLOGY

## **The promotor and poison effects of the inorganic elements of kraft lignin during hydrotreatment over nimos catalyst**

Downloaded from: <https://research.chalmers.se>, 2021-08-31 11:14 UTC

Citation for the original published paper (version of record):

Sebastian, J., Cheah, Y., Bernin, D. et al (2021)

The promotor and poison effects of the inorganic elements of kraft lignin during hydrotreatment over nimos catalyst

Catalysts, 11(8)

<http://dx.doi.org/10.3390/catal11080874>

N.B. When citing this work, cite the original published paper.

## Article

# The Promotor and Poison Effects of the Inorganic Elements of Kraft Lignin during Hydrotreatment over NiMoS Catalyst

Joby Sebastian <sup>1</sup>, You Wayne Cheah <sup>1</sup>, Diana Bernin <sup>2</sup>, Derek Creaser <sup>1</sup>  and Louise Olsson <sup>1,\*</sup> 

<sup>1</sup> Competence Center for Catalysis, Chemical Engineering, Chalmers University of Technology, SE-412 96 Gothenburg, Sweden; joby@chalmers.se (J.S.); cheah@chalmers.se (Y.W.C.); derek.creaser@chalmers.se (D.C.)

<sup>2</sup> Department of Chemistry and Chemical Engineering, Chalmers University of Technology, SE-412 96 Gothenburg, Sweden; diana.bernin@chalmers.se

\* Correspondence: louise.olsson@chalmers.se

**Abstract:** One-pot deoxygenation of kraft lignin to aromatics and hydrocarbons of fuel-range quality is a promising way to improve its added value. Since most of the commercially resourced kraft lignins are impure (Na, S, K, Ca, etc., present as impurities), the effect of these impurities on the deoxygenation activity of a catalyst is critical and was scrutinized in this study using a NiMoS/Al<sub>2</sub>O<sub>3</sub> catalyst. The removal of impurities from the lignin indicated that they obstructed the depolymerization. In addition, they deposited on the catalyst during depolymerization, of which the major element was the alkali metal Na which existed in kraft lignin as Na<sub>2</sub>S and single-site ionic Na<sup>+</sup>. Conditional experiments have shown that at lower loadings of impurities on the catalyst, their promotor effect was prevalent, and at their higher loadings, a poisoning effect. The number of moles of impurities, their strength, and the synergism among the impurity elements on the catalyst were the major critical factors responsible for the catalyst's deactivation. The promotor effects of deposited impurities on the catalyst, however, could counteract the negative effects of impurities on the depolymerization.

**Keywords:** lignin; kraft pulping; NiMoS catalyst; deoxygenation; deactivation; lignin pretreatment



**Citation:** Sebastian, J.; Cheah, Y.W.; Bernin, D.; Creaser, D.; Olsson, L. The Promotor and Poison Effects of the Inorganic Elements of Kraft Lignin during Hydrotreatment over NiMoS Catalyst. *Catalysts* **2021**, *11*, 874. <https://doi.org/10.3390/catal11080874>

Academic Editors: Hwai Chyuan Ong, Chia-Hung Su and Hoang Chinh Nguyen

Received: 24 June 2021  
Accepted: 16 July 2021  
Published: 21 July 2021

**Publisher's Note:** MDPI stays neutral with regard to jurisdictional claims in published maps and institutional affiliations.



**Copyright:** © 2021 by the authors. Licensee MDPI, Basel, Switzerland. This article is an open access article distributed under the terms and conditions of the Creative Commons Attribution (CC BY) license (<https://creativecommons.org/licenses/by/4.0/>).

## 1. Introduction

Lignin valorization can improve the economic viability of a lignocellulosic biorefinery. Biofuel synthesis from industrial lignin streams (technical lignins) is a promising way to address the fuel sustainability footprint and the economics of the pulp and paper industries [1–7]. For instance, approximately 75,000 tons of kraft lignin were produced globally in 2015, and it is anticipated to surpass 250,000 tons by 2025 [8]. At present, most of the kraft lignin produced is reintegrated back into the kraft pulping process as a combustion fuel to generate the process energy. This leads to its low added value (\$70–150 per ton) [8–10]. Depolymerization of lignins to monomeric oxygenates, such as phenols, can significantly improve the lignin value addition (approximately \$1300 per ton) [8,11]. Lignin depolymerization accompanied with hydrodeoxygenation (HDO) generates a product mixture composed of aromatics and hydrocarbons suitable for fuel and fuel additives [1,3,6,12,13].

Catalytic hydrotreatment of lignin to monomers using solid catalysts is a widely implemented method in lignin valorization [14–20]. One of the crucial factors that affect the life of a catalyst in biomass processing is the purity of the feedstocks [5,21]. Contaminants in the feedstocks can act as poisons to the active sites, gradually decreasing their activity and selectivity during the time-on-stream. Once poisoned, many of the catalysts cannot be regenerated, for instance, Ru/TiO<sub>2</sub> in the hydrogenation of sugars [22] and CoMoS/MgAl<sub>2</sub>O<sub>4</sub> in the hydrolysis of biomass [23,24], necessitating the use of fresh catalysts, henceforth affecting the economics of the entire process. The kraft process involving NaOH and Na<sub>2</sub>S reagents leaves the byproduct lignin with a substantial amount of impurities, such as Na and S, along with the other inorganic impurities from the source wood (e.g., Si, K, Ca,

and Fe) [25–27]. Hence, during the depolymerization and deoxygenation of kraft lignin over solid catalysts, the above impurities (Na, S, K, Ca, Fe, etc.) are highly expected to deteriorate the performance of the catalyst [5].

In most of the studies related to the catalytic valorization of lignin, much emphasis has been given to the lignin depolymerization mechanism, the product analysis, and the catalyst structure–activity correlations [15,17–20,28,29]. But for operation in industrial applications, it is critical to also study the long-term stability, deactivation, and regeneration of the catalysts. Especially since the feedstock is continuously fed to the catalyst, and the catalyst undergoes occasional thermal regenerations to burn off the coke [5].

However, the performance of a typical HDO catalyst, such as NiMoS/Al<sub>2</sub>O<sub>3</sub>, in consecutive kraft lignin HDO runs, especially after its thermal regeneration, to investigate the deposition of impurities from the lignin to the catalyst, and the role of these impurities on the catalytic activity has, to our knowledge, not been studied. This was the objective of the current study. Herein, the effect of these inorganic impurity elements of kraft lignin on the deoxygenation activity of a NiMoS/Al<sub>2</sub>O<sub>3</sub> catalyst during subsequent runs is reported. Elemental analysis of the kraft lignin showed significant amounts of the above impurity elements. Recycle studies were performed with thermally regenerated catalysts to verify the deposition of these impurities on the catalyst. To understand and differentiate the extent of the negative effect of different impurities (Na, K, Ca, and Fe) towards deoxygenation, catalysts containing different amounts of individual impurities were used for the hydrotreatment. The correlation of the quantity and strength of impurities on the product yield, deoxygenation activity, and solid residue amount was investigated. Finally, to remove the impurities of the kraft lignin, the lignin was subjected to a dilute acetic acid washing treatment. The pretreated lignin was characterized both elementally and structurally. The product yield obtained over the pretreated lignin was compared with the untreated lignin to reveal the benefits of the pretreatment.

## 2. Results and Discussion

### 2.1. Lignin Characterization

Kraft lignin was used as the feedstock for this study (Sigma Aldrich, product no: 370959, Supplementary Materials, Materials S1). The 2D heteronuclear single-quantum coherence nuclear magnetic resonance (HSQC NMR) analysis of the lignin showed mainly the presence of guaiacol units (G units), indicating that the lignin had a softwood origin. Table 1 provides the elemental composition of the kraft lignin. A significant amount of S (2.1 wt%), Na (0.93 wt%), Si (0.60 wt%), and K (0.11 wt%) was found in the lignin with minor amounts of Ca, Mn, Fe, B, Mg, and Al (0.02–0.0018 wt%), and many more elements were present at levels less than 0.0018 wt% (Table S2). The large contribution of Si in lignin was most likely from the wood source [30,31]. The ash content of the lignin was approximately 1.64 wt% according to the thermogravimetric analysis (Figure S2). Based on the CHNS analysis, the C, H, N, and S contents of the lignin were 62.1, 5.8, 0.4, and 2.2 wt%, respectively, (C/H = 10.6, C/S = 28.5).

### 2.2. Catalytic Activity during Hydrotreatment

Hydrotreatment of kraft lignin in the presence of the NiMoS/Al<sub>2</sub>O<sub>3</sub> catalyst produced a colorless transparent liquid product (Figure 1B inset). The GC × GC analysis of this product solution did not show any peaks indicative of oxygenates (Figure 1B, compare Figure 1A for the classification of different compounds). The NiMoS/Al<sub>2</sub>O<sub>3</sub> is active for the deoxygenation reaction under the chosen experimental conditions. Many cycloalkanes (various substituted cyclohexanes), and deoxygenated aromatics (benzene and naphthalene derivatives) were observed in the chromatogram (Figure S3 provides the product identification). The yield of cycloalkanes and aromatics were 10.9 wt% and 0.76 wt% respectively (Figure 2). The amount of solid residue generated after the reaction was 41.4 wt% (C/H = 18.3, C/S = 19.5). This amount is similar to that reported in the presence of dodecane solvent [29]. An increase in the C/H ratio in the solid residue as compared to

the feedstock kraft lignin indicates the formation of more recalcitrant C–C bonds through condensation/polymerization during the depolymerization. A blank run without the catalyst but only using kraft lignin generated 57 wt% of solid residue, and the product mixture was entirely composed of oxygenates. Indeed, the catalyst was essential to reduce the solid residue and to produce the targeted hydrocarbon products.

**Table 1.** Elemental analysis of the kraft lignin and the pretreated kraft lignin.

Elements <sup>a</sup>	Kraft Lignin (ppm)	Pretreated Kraft Lignin (ppm)
S	21,000	9000
Na	9300	28
Si	6000	<100
K	1100	5
Ca	200	7
Mn	58	1.7
Fe	30	24
B	22	4
Mg	21	9
Al	18	125

<sup>a</sup> Detected above 15 ppm in kraft lignin.

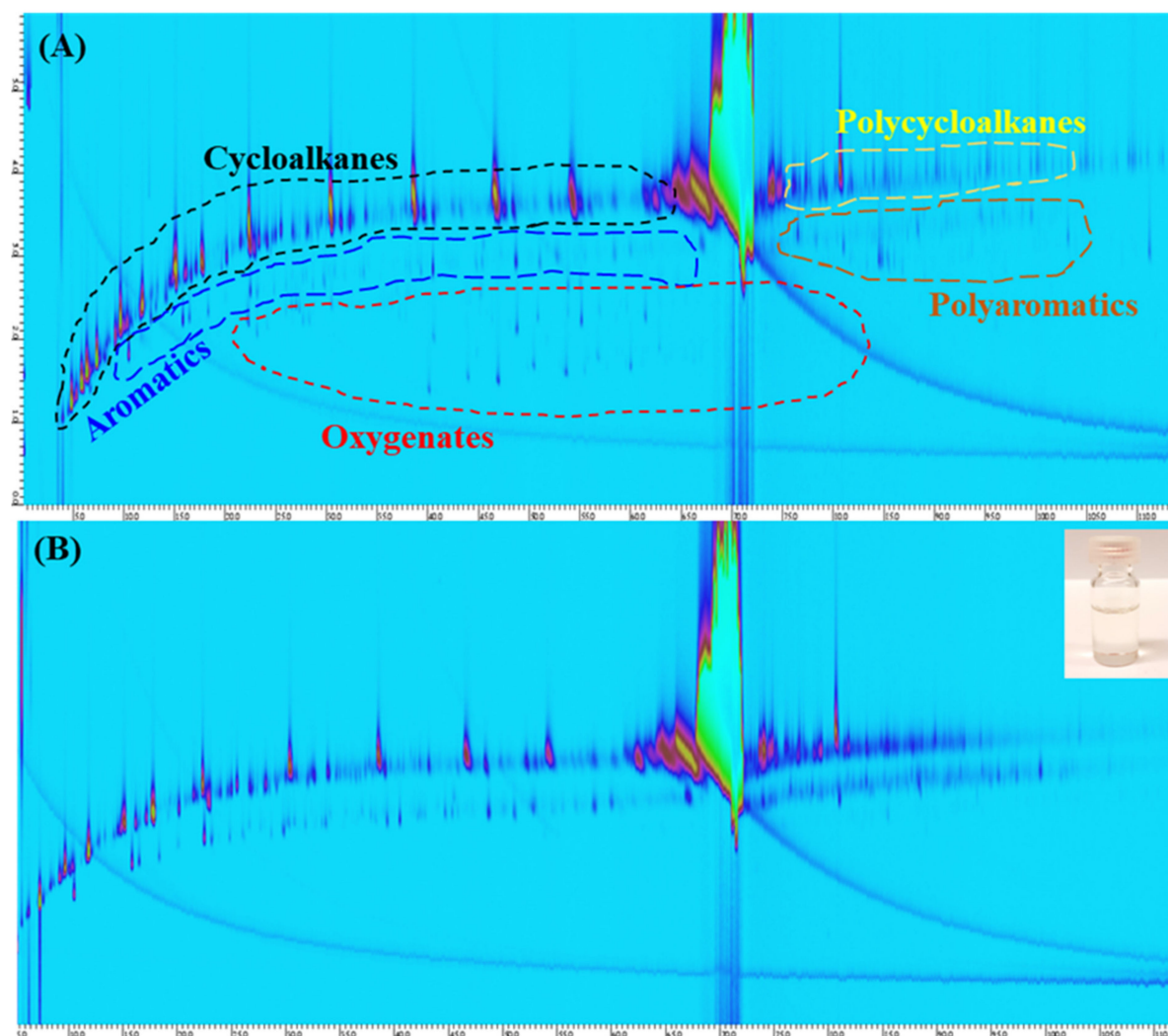


**Figure 1.** GC × GC chromatogram of reaction products: (A) classification of different compounds; (B) reaction over NiMoS/Al<sub>2</sub>O<sub>3</sub> catalyst; inset shows an image of the liquid product.

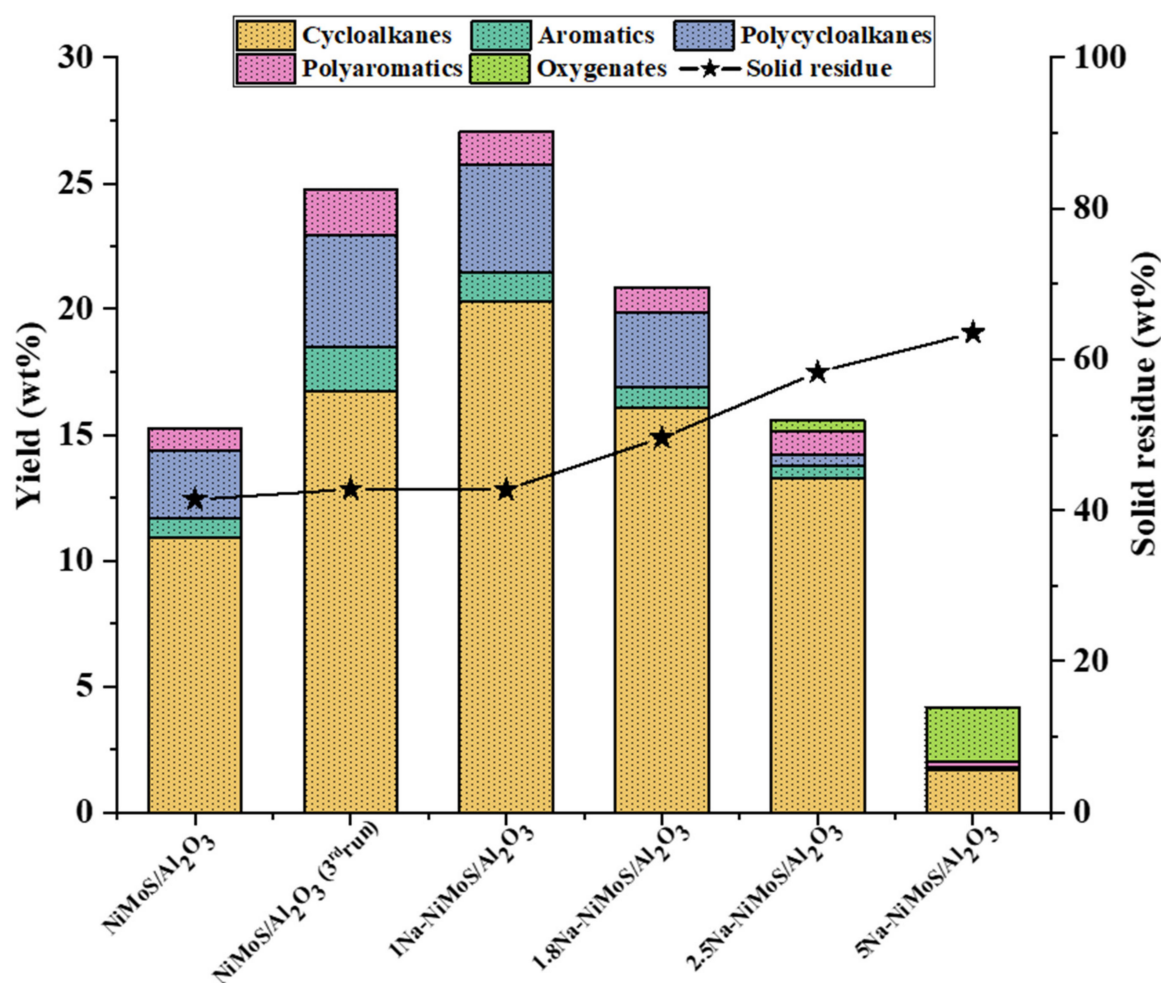


Figure 2. Product yield and solid residue obtained over NiMoS/Al<sub>2</sub>O<sub>3</sub> containing different amounts of Na.

### 2.3. Recycle Studies

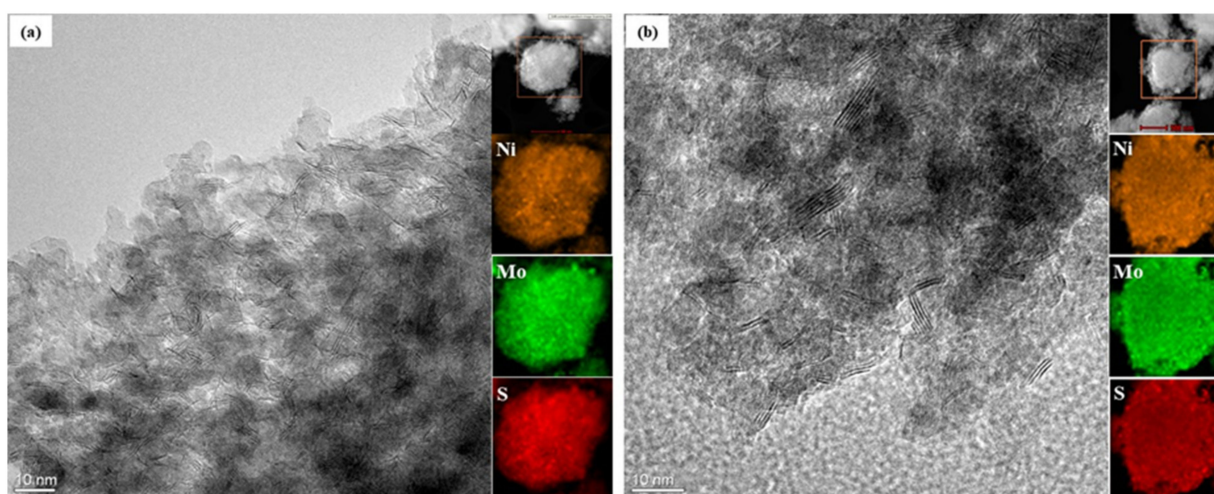
Recycle studies on NiMoS/Al<sub>2</sub>O<sub>3</sub> were performed to establish the deposition of the inorganic impurities from the lignin to the catalyst during the depolymerization. The carbon deposition on the catalyst after a single run was 0.75 wt%, and the sulfur reduction was 1.5 wt%. Therefore, before the recycle runs, the catalyst was oxidized and freshly sulfided (Supplementary Materials, Recycle experiments S6). Thermal activation/rejuvenation of catalysts is a common practice in many industrial processes [5]. Two recycles were done to achieve a significant deposition of the impurities on the catalyst. The elemental analysis of the catalyst after its 2nd recycle (i.e., 3rd run) showed a significant amount of Na (357 ppm), K (180 ppm), Ca (180 ppm), and Fe (183 ppm) (Table 2) on it. This confirms that the impurities of kraft lignin were deposited on the catalyst during the depolymerization thus changing its composition. The remaining quantity of impurities was found in the solid residue (Table 2). One advantage of generating a small amount of solid residue during the hydrotreatment of kraft lignins appears to be that the residue could minimize the deposition of impurities on the catalysts. Moreover, the solid residue can be utilized via the reforming reaction [32], in the synthesis of composite materials [33], and as a soil conditioner [34], consequently improving its value addition. However, it is of course important to minimize the solid residues in order to increase the bio-oil yield.



**Table 2.** Elemental analysis of the NiMo/Al<sub>2</sub>O<sub>3</sub> catalyst before the hydrotreatment, after the 3rd run, and the solid residue generated after the 3rd consecutive run.

Element	Fresh Catalyst (ppm)	After 3rd Run (ppm)	Solid Residue (ppm)
Ni	38,500	38,500	72
Mo	111,000	104,000	90
Na	<50	357	15,400
Ca	<50	180	600
K	<30	180	1550
Fe	114	183	233
Si	<200	<200	<500
Mn	10.5	15.4	96

The catalyst after its 3rd run was characterized to analyze the morphological changes that occurred during the recycle experiments. The Ni, Mo, and S distribution on the catalyst after the 3rd run was found to be fairly uniform as that of the fresh catalyst (Figure 3). The Mo concentration was quite similar, but slightly lower after three runs, which could indicate a small amount of leaching, but it could also be within the accuracy of the ICP measurement. The average MoS<sub>2</sub> slab length increased from approximately 5.4 nm in the fresh catalyst to 16.9 nm after its 3rd run. Likewise, the average number of MoS<sub>2</sub> slabs (the thickness) increased from approximately 2.7 to 13.2. This could be attributed to the repeated thermal treatments, the deposition of impurities on the catalyst, and the redistribution of the active components on the catalyst during the hydrotreatment. In essence, the MoS<sub>2</sub> dispersion on the support decreased which was likely to reduce the activity of the catalyst.

**Figure 3.** HRTEM images showing the MoS<sub>2</sub> fringes and the elemental distribution of NiMoS/Al<sub>2</sub>O<sub>3</sub>: (a) fresh and (b) after the 3rd consecutive run.

However, the GC × GC analysis of the liquid product generated after the 3rd run of the catalyst did not show any oxygenates (chromatogram, Figure S4). In addition, the yields of cycloalkanes and aromatics were higher than the first run. The cycloalkanes yield increased to 16.7 wt% from its 1st run (10.9 wt%), and the aromatics yield increased to 1.8 wt% from 0.76 wt% (Figure 2). This catalytic behavior is most likely then attributable to the change in the composition of the catalyst, i.e., due to the positive effect of the impurities (approximately 0.09 wt% in total on the catalyst, from Table 2); however, the contribution from other structural/electronic properties of the catalyst arising from the repeated thermal treatments could not be completely ruled out. On the other hand, the solid residue generated (42.8 wt%) after the 3rd run was 1.4 wt% higher than from its 1st run (Figure 2), indicating that the impurities, if accountable, may have a minor negative effect on lignin conversion to liquid products.

To validate the positive and negative effects of the impurity elements (compositional effects), more importantly, their individual effects, on the activity of a thermally regenerated catalyst, conditional experiments were performed with catalysts containing different amounts of individual impurity elements.

#### 2.4. Effect of the Amount of Na on the Activity of NiMoS/Al<sub>2</sub>O<sub>3</sub> Catalyst

The major inorganic impurity element, apart from S, that existed in the kraft lignin is the alkali metal Na (0.93 wt%, Table 1). The amount of the next dominant impurity elements such as K, Ca, and Fe were 8.5, 46.5, and 310 times lower than Na. Consequently, Na can be considered as the first element that could influence the deoxygenation activity of the catalyst. The Na was the dominant impurity element deposited on the catalyst after its 3rd run too (Table 2). To study the effect of the amount of Na on the activity of the NiMoS/Al<sub>2</sub>O<sub>3</sub>, catalysts containing 1–5 wt% of Na (Supplementary Materials, Catalyst synthesis S2) were used for the hydrotreatment.

Over the 1Na–NiMoS/Al<sub>2</sub>O<sub>3</sub> (contains 1 wt% of Na) catalyst, the yield of cycloalkanes and aromatics were 20.3 wt% and 1.1 wt%, respectively (Figure 2). It was almost 9.4 wt% and 0.4 wt%, respectively, higher than that obtained over the catalyst without any Na (NiMoS/Al<sub>2</sub>O<sub>3</sub>). This confirms that Na can increase the deoxygenation performance of the catalyst. The Na appears to act as a promotor for the NiMoS/Al<sub>2</sub>O<sub>3</sub> catalyst. The positive effect of alkali elements on the activity of MoS<sub>2</sub> based catalysts is known in the literature [35]. The performance of the 3rd run catalyst (contains a total of approximately 0.09 wt% impurities, from Table 2) falls in between NiMoS/Al<sub>2</sub>O<sub>3</sub> and 1Na–NiMoS/Al<sub>2</sub>O<sub>3</sub> (Figure 2).

An increase in the amount of Na on the catalyst to 1.8 wt% from 1 wt% (1.8Na–NiMoS/Al<sub>2</sub>O<sub>3</sub>) decreased the cycloalkanes and aromatics yields to 16.1 wt% and 0.82 wt%, respectively (Figure 2), but, still, the liquid product yields were better than for the NiMoS/Al<sub>2</sub>O<sub>3</sub> alone. The promotor effect of Na appeared to be high when present in ≤1wt% on the catalyst.

A further increase in the amount of Na on the catalyst to 2.5 wt% (2.5Na–NiMoS/Al<sub>2</sub>O<sub>3</sub>) decreased the cycloalkanes and aromatics yield to 13.3 wt% and 0.46 wt%, respectively (Figure 2). Yet, the catalyst's performance was better than the NiMoS/Al<sub>2</sub>O<sub>3</sub> alone when considering the cycloalkanes and aromatics yields, but its performance was not better considering the overall product yield. Moreover, with this amount of Na on the catalyst, oxygenates started to remain in the product mixture (0.4 wt% in yield) (chromatogram, Figure S5). A higher amount of Na (1.8 wt%) on the catalyst decreased the deoxygenation activity of the catalyst.

An additional increase in the Na amount to 5 wt% on the catalyst (5Na–NiMoS/Al<sub>2</sub>O<sub>3</sub>) significantly reduced the cycloalkanes yield to merely 1.7 wt% and the aromatics yield to 0.13 wt% (Figure 2). In contrast, the oxygenates yield increased to 2.2 wt%.

The effect of the amount of Na on the product yield follows a volcanic correlation with its amount. The promotional effect of Na was observed at its lower amounts (≤1wt%), above which poisoning effects were initiated.

On the other hand, the solid residues generated after the hydrotreatments increased with an increase in the amount of Na on the catalyst (Figure 2). It was 42.7 wt% over the 1Na–NiMoS/Al<sub>2</sub>O<sub>3</sub> catalyst (compared to 41.1 wt% in the case of fresh NiMoS/Al<sub>2</sub>O<sub>3</sub>), while it increased to 63.5 wt% over the 5Na–NiMoS/Al<sub>2</sub>O<sub>3</sub> catalyst. A higher amount of Na on the catalyst increased the solid residue formation rate, hence, validating the positive and negative effects of the Na impurity.

#### 2.5. Effect of Other Impurities on the Activity of NiMoS/Al<sub>2</sub>O<sub>3</sub>

The 2.5 wt% was the minimum amount of Na on NiMoS/Al<sub>2</sub>O<sub>3</sub> that resulted in the retention of oxygenates in the product mixture. To compare the effect of Na, K, Ca, and Fe on the activity of the catalyst, NiMoS/Al<sub>2</sub>O<sub>3</sub> containing 2.5 wt% of individual

impurities (2.5K–NiMoS/Al<sub>2</sub>O<sub>3</sub>, 2.5Ca–NiMoS/Al<sub>2</sub>O<sub>3</sub>, and 2.5Fe–NiMoS/Al<sub>2</sub>O<sub>3</sub>) were used for the hydrotreatment.

Over the 2.5K–NiMoS/Al<sub>2</sub>O<sub>3</sub> catalyst, a higher yield of cycloalkanes and aromatics, 14.4 wt% and 0.80 wt%, respectively, as compared to 2.5Na–NiMoS/Al<sub>2</sub>O<sub>3</sub> was obtained (Figure 4). These yields were 1.1 wt% and 0.34 wt% higher than the 2.5Na–NiMoS/Al<sub>2</sub>O<sub>3</sub> catalyst. The 2.5Ca–NiMoS/Al<sub>2</sub>O<sub>3</sub> catalyst also showed an increase in cycloalkanes and aromatics yields (an increase of 4.8 wt% and 0.84 wt%, respectively, for cycloalkanes and aromatics) as compared to 2.5Na–NiMoS/Al<sub>2</sub>O<sub>3</sub> (Figure 4). The 2.5Fe–NiMoS/Al<sub>2</sub>O<sub>3</sub> catalyst likewise gave a 5.5 wt% increase in cycloalkanes yield and 1.1 wt% increase in aromatics yield as compared to the 2.5Na–NiMoS/Al<sub>2</sub>O<sub>3</sub> catalyst. These yields were higher than the catalyst without any impurities (NiMoS/Al<sub>2</sub>O<sub>3</sub>), further confirming the promoter effect of K, Ca, and Fe. No oxygenates were retained in the product mixture with these catalysts containing impurities. These elements (K, Ca, and Fe), when present at the same amount (2.5 wt%) as Na, turned out to be promoters rather than poisons.

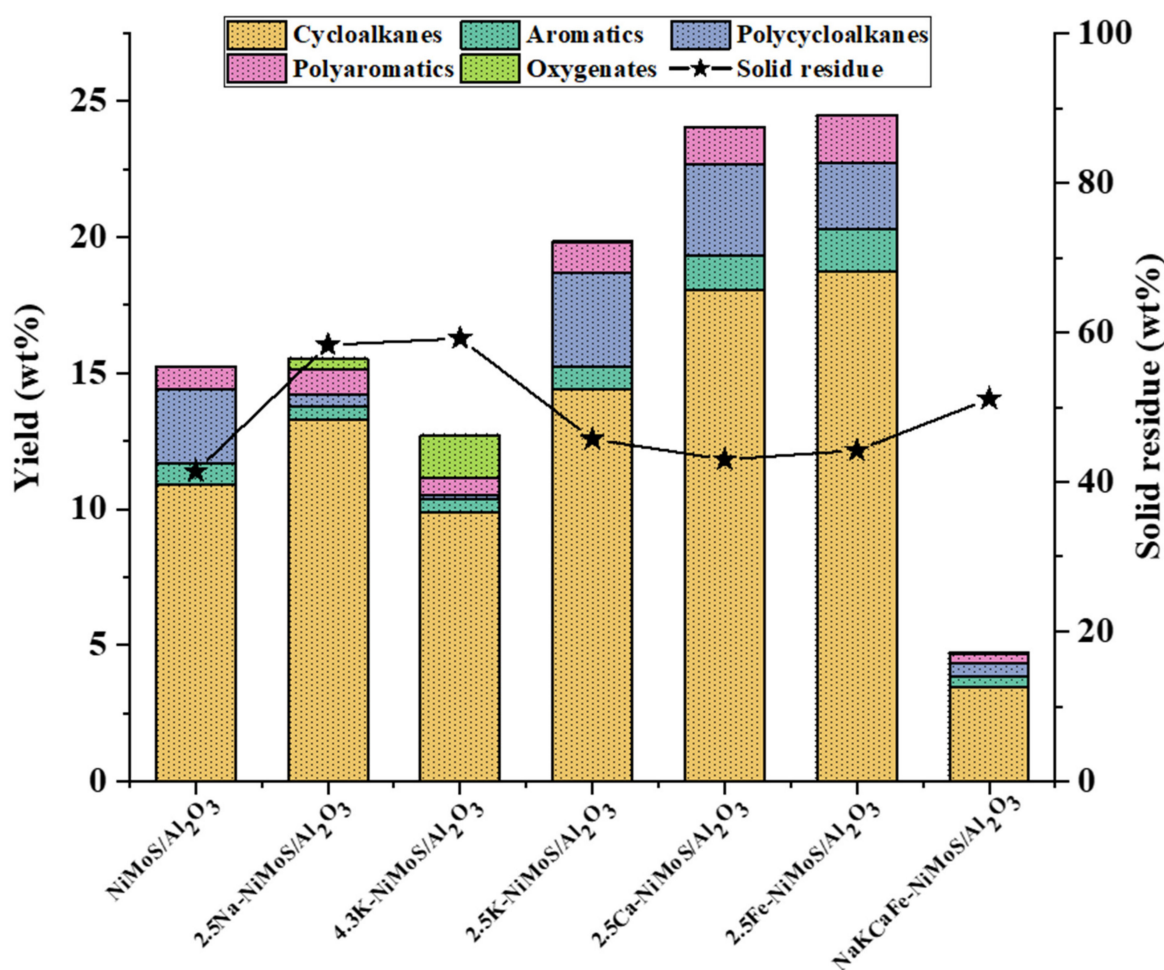


**Figure 4.** Comparison of activity of NiMoS/Al<sub>2</sub>O<sub>3</sub> catalysts containing different impurities.

The solid residue generated over these catalysts were 45.7 wt%, 43.0 wt%, and 44.2 wt%, respectively, for K, Ca, and Fe, significantly lower than the 2.5 wt% of the Na-containing catalyst (58.3 wt%) (Figure 4), but only marginally higher than for NiMoS/Al<sub>2</sub>O<sub>3</sub> alone (41.1 wt%). Theoretically, the lignin amount that would deposit 2.5 wt% Na on the catalyst would result in only the deposition of 0.286 wt% of K, 0.052 wt% of Ca, and 0.0078 wt% of Fe on the catalyst (Table 1). The increase in the product yield and solid residue after the 3rd run of the catalyst was therefore due to the lower amount of deposition of impurities on it. The lower amount facilitated their promoting role on the catalyst.



Apart from the amount (mass), the molar amount of impurity elements could also be a contributing factor to the deactivation of the catalyst. The molar masses of K, Ca, and Fe were higher than Na. Hence, the number of moles present on the catalyst at their equal wt% (2.5 wt%) followed the order Na > K > Ca > Fe. We, therefore, examined an equal number of moles of K (4.3K–NiMoS/Al<sub>2</sub>O<sub>3</sub>) as compared to 2.5 wt% of Na on the catalyst. The 4.3K–NiMoS/Al<sub>2</sub>O<sub>3</sub> catalyst gave only 9.9 wt% yields to cycloalkanes (Figure 4), which was 3.4 wt% lower than that obtained over the catalyst containing the same number of moles of Na (2.5Na–NiMoS/Al<sub>2</sub>O<sub>3</sub>). The aromatics yield was almost the same, 0.5 wt%. Moreover, the catalyst gave a 1.6 wt% yield to oxygenates, was almost 1.2 wt% higher than the 2.5Na–NiMoS/Al<sub>2</sub>O<sub>3</sub> catalyst. Thus, the K impurity had a much stronger negative effect on the deoxygenation activity of the catalyst than Na. In addition, similar to the Na, an increase in the amount of the K on the catalyst decreased the lignin product yield (Figure 4, compared to 2.5K–NiMoS/Al<sub>2</sub>O<sub>3</sub> and 4.3K–NiMoS/Al<sub>2</sub>O<sub>3</sub>). At a lower amount of K, its promotor effect was more dominating than its poisoning effect. Hence, the 180 ppm of K deposited on the catalyst after its 3rd run (Table 2) will likely have a promotor effect rather than a poisoning effect. This study also indicates that the number of moles of impurity elements on the lignin is also important apart from their amount (wt%) in deactivating the catalyst. Since Na was the lowest molecular weight impurity element present in a higher amount in our feedstock (the highest number of moles), it will be the first element that will be initiating the promotional and eventual deactivation effects on the catalyst.

The synergism among different impurity elements on the activity of the catalyst can also be a contributing factor. This was studied by taking a single NiMoS/Al<sub>2</sub>O<sub>3</sub> catalyst containing 1.8 wt% of Na, 0.22 wt% of K, 0.04 wt% of Ca, and 0.01 wt% of Fe, designated as NaKCaFe–NiMoS/Al<sub>2</sub>O<sub>3</sub>. These amounts (a total of 2.07 wt%) were derived based on the assumption of the complete conversion of the lignin without any formation of the solid residue in a single run. The cycloalkanes yield obtained over this catalyst was only 3.5 wt%, and the aromatics yield was 0.37 wt% (Figure 4). These yields are significantly lower than that of the catalyst containing only 2.5 wt% of Na (2.5Na–NiMoS/Al<sub>2</sub>O<sub>3</sub>), implying that, when all of these impurity elements are present together on the catalyst, the deactivation is much faster. Therefore, apart from the amount and number of moles of the impurity elements, the synergism between them is also responsible for the deactivation of the catalyst. The higher activity of the 3rd run catalyst, when all these elements were present indicates that, at their lower amount (Table 2), they act as promotors. The solid residue obtained over the NaKCaFe–NiMoS/Al<sub>2</sub>O<sub>3</sub> was 50.1 wt%, higher than any of the individual catalysts or the catalyst after the 3rd run.

The most efficient way for lignin valorization is not to generate any solid lignin residue. Based on the above observations, at our experimental conditions, assuming that no solid residue was generated during the hydrotreatment, the catalyst would very likely deactivate after a single run. In NiMoS/Al<sub>2</sub>O<sub>3</sub>-based catalytic systems, the extent of deactivation will depend on the amount of solid residue generated (depends on the experimental conditions) and on the lignin-to-catalyst ratio.

Since the composition of inorganic elements in lignin varies based on the wood source, the pulping process, and the lignin extraction method, this study laid out an overall depiction of the effect of impurities on the deoxygenation activity of a NiMoS/Al<sub>2</sub>O<sub>3</sub> catalyst, and the potential promotors for the catalyst when impurity-free lignins are used as the feedstocks.

## 2.6. The Chemical Nature of Na in Kraft Lignin

Since Na was the major impurity element present in the lignin, <sup>23</sup>Na MAS NMR analysis on kraft lignin was performed to understand its chemical nature. The NMR spectrum shown in Figure 5 has two signals, one sharp signal at −0.796 ppm and a broad signal at −7.75 ppm. The broad signal at −7.75 ppm with no quadrupolar pattern indicates the absence of well-crystallized Na [36]. Hence, this signal can arise from a

situation where the  $\text{Na}^+$  ions are not present in a well-defined crystalline structure or, more specifically, as a one-site ionic form similar to that observed in dehydrated Na-zeolites [37] and Na exchanged sulfonated polystyrenes [38]. The isotropic line shape close to 0 ppm (at  $-0.796$  ppm) was due to Na in a cubic symmetry. Since  $\text{Na}_2\text{S}$  has a cubic crystal structure, the NaOH crystals are of orthorhombic symmetry, and the  $\text{Na}_2\text{SO}_4$  crystals are of orthorhombic (anhydrous) and monoclinic (hydrated) symmetries, this signal can be assigned to the residual  $\text{Na}_2\text{S}$  left on the lignin from the kraft pulping process.

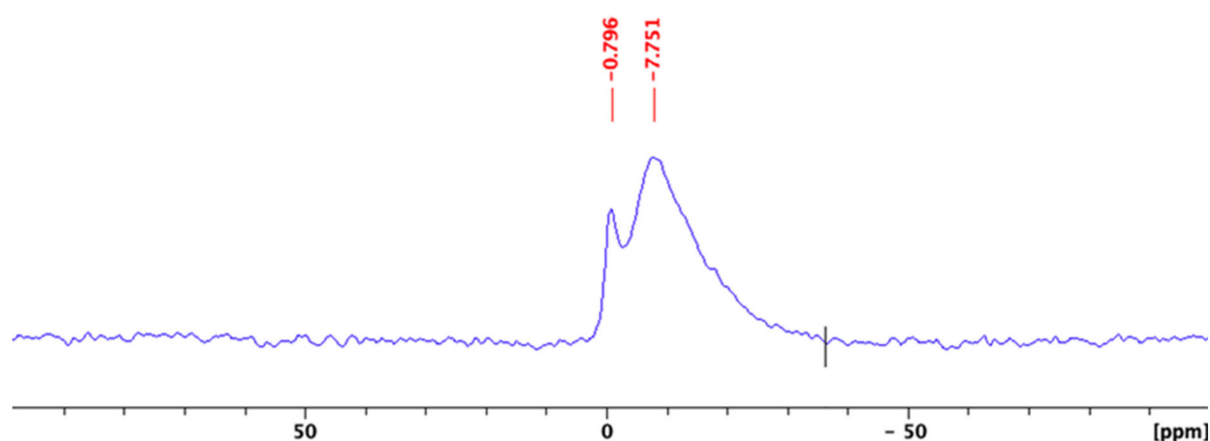


**Figure 5.**  $^{23}\text{Na}$  MAS NMR spectrum of kraft lignin.

It is thus possible to remove the majority of  $\text{Na}^+$  ions by simple ion exchange with protic acids. The acid treatment could also be helpful to remove the residual  $\text{Na}_2\text{S}$  on the lignin.

### 2.7. Pretreatment of Kraft Lignin

It is essential to remove the impurities from the lignin to improve the stability of the catalyst for hydrotreatments involving multiple runs where the catalyst undergoes regeneration treatments, or with the continuous feeding of the feedstock. Acid washing is a widely followed method used for lignin purification. In general, any further treatment of lignin is likely to modify its structure, especially the aggravation of condensation reactions to generate more recalcitrant C–C bonds [39,40]. In this study, a very dilute acetic acid solution (5 vol%) was used as the leaching medium in a batch process [39,40]. Acetic acid is sustainable, as it is produced during the pyrolysis of lignocellulosic biomass [41]. The pretreatment temperature was set at  $85\text{ }^\circ\text{C}$  and the pretreatment time was for 1 h (Supplementary Materials, Pretreatment of kraft lignin S8). The condensation of lignin during acetic acid treatment in a batch process is somewhat unavoidable (vide infra).

#### 2.7.1. Characterization of Pretreated Lignin

Table 1 shows the elemental analysis of the pretreated kraft lignin after the pretreatment. Most of the inorganic impurities were removed to low levels. For instance, the Na content decreased from 9300 ppm in the fresh lignin to merely 28 ppm in the pretreated lignin. The number of other impurities, such as K and Ca, decreased to minor levels of 5 and 7 ppm, respectively (Table S3 provides the concentrations of all the elements). The C, H, N, and S contributions of the lignin were 64.7, 6.3, 0.06, and 1.3 wt%, respectively. As compared to the untreated kraft lignin, the C/H ratio of pretreated kraft lignin only marginally decreased from 10.6 to 10.3. However, the C/S ratio showed a large difference.

It increased to 50.7 from 28.5 after the pretreatment due to the sulfur removal, possibly via the  $\text{Na}_2\text{S}$ . The 2D HSQC NMR analysis of the fresh and pretreated lignin indicated an increase in the contribution of C–C bonds after the pretreatment (Figures S6 and S7). For example, the integral ratio of  $-\text{OMe}$  to aromatic signals ( $G_2 + G_5 + G_6$ ) was increased from 0.65 for untreated lignin to 1.57 for pretreated lignin. The higher ratio in pretreated lignin

indicates that the C<sub>2</sub>, C<sub>5</sub>, and C<sub>6</sub> of G<sub>2</sub>, G<sub>5</sub>, and G<sub>6</sub> units underwent condensation reactions by sacrificing their C<sub>2</sub>, C<sub>5</sub>, and C<sub>6</sub> hydrogen atoms. In essence, the acid pretreatment was efficient in removing the impurities of kraft lignin, but it modified the lignin structure.

### 2.7.2. Hydrotreatment of Pretreated Lignin

Hydrotreatment of the pretreated kraft lignin over the NiMoS/Al<sub>2</sub>O<sub>3</sub> catalyst resulted in an overall increase in the product yields (Figure 6). Especially, the cycloalkanes yield increased to 19.7 wt%, almost an 8.8 wt% increase as compared to the untreated lignin. Similarly, the aromatics yield also increased to 1.8 wt% (a 1.1 wt% increase as compared to the aromatics yield from the untreated lignin). These results point out that the impurities themselves have different roles (in the presence of the catalyst) when present in the lignin and when present on the catalyst. When they are absent in the lignin, such as the pretreated lignin in the present study, their negative role vanishes, and the catalyst's performance dominates. In contrast, when they are present in the lignin (the untreated kraft lignin), their effect perhaps dominates the catalytic effects. For instance, the K impurity from beech wood was found to catalyze the polymerization reaction during the hydroprocessing [24]. Since these impurities are in direct contact with or coordinated to (Figure 5) the lignin, during the depolymerization, their effect on the lignin would be stronger than the catalyst's effect on the depolymerized oligomers. This dominant effect can be overcome either by increasing the catalyst amount or by using a more active catalyst, such as the promoted catalysts in the present study (i.e., 1Na–NiMoS/Al<sub>2</sub>O<sub>3</sub>, 2.5(K, Ca, or Fe)–NiMoS/Al<sub>2</sub>O<sub>3</sub>). For instance, the same product yield from pretreated lignin can also be obtained from the untreated lignin by using the promoted 1Na–NiMoS/Al<sub>2</sub>O<sub>3</sub> catalyst (compare Figures 4 and 6). However, during catalyst recycle/continuous runs, additional impurities will be deposited on the promoted catalyst. Thermal reactivation of the catalysts before the next run can change their electronic effects (synergism) and distribution on the catalyst, aggravating their poisoning effects. Hence, there is a limit to fine-tuning the activity of the catalysts by promoting when using untreated lignin. In contrast, lignin pretreatment has the benefits of avoiding the negative effects of impurities on depolymerization and the longer-term negative effects with high deposition on the catalyst. The net effect is longer catalyst life and higher product yield.

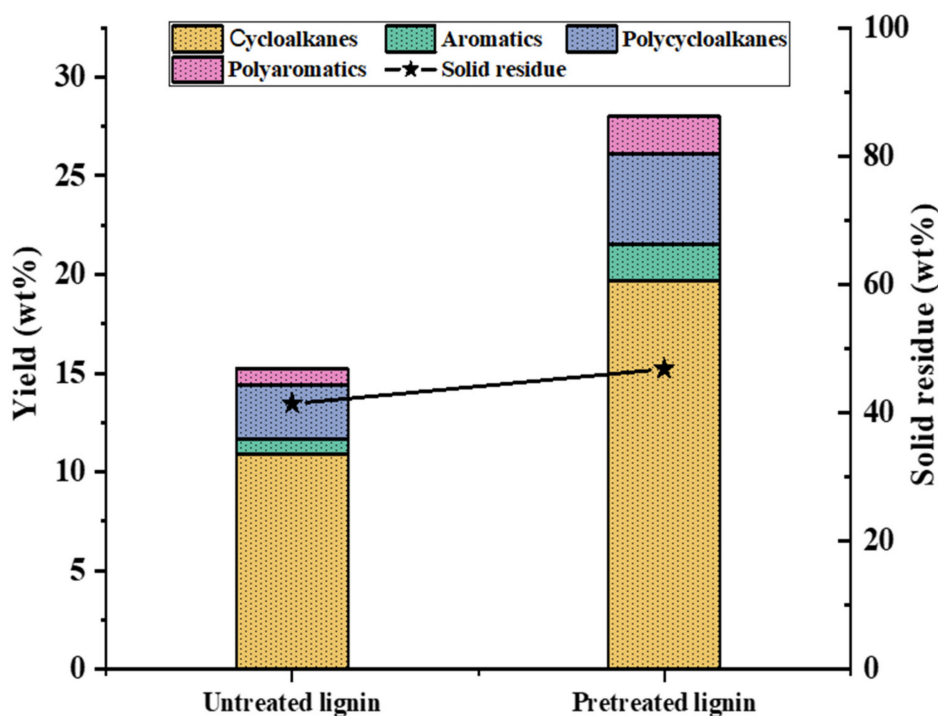


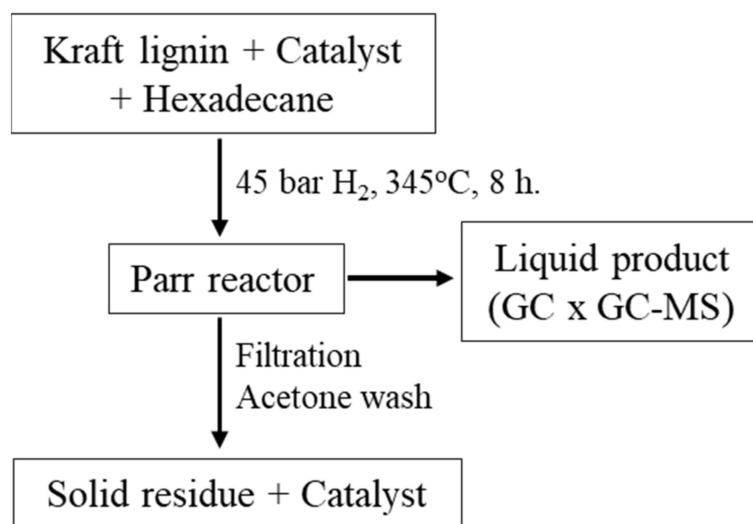
Figure 6. Product yield and solid residue obtained with untreated and pretreated lignins over the NiMoS/Al<sub>2</sub>O<sub>3</sub> catalyst.

The solid residue generated after the reaction was 46.8 wt% (C/H = 15.6 and C/S = 38.9), which was almost 5.4 wt% higher than the untreated lignin. This increase can be correlated to the increase in the C–C bond fraction of the lignin that occurred during the acid pretreatment. The gain in product yield outweighs the increase in solid residue amount.

Based on the previous observations, it can be presumed that the yield of cycloalkanes and aromatics from pretreated lignin could be further improved by using Na-, K-, Ca-, or Fe–NiMoS/Al<sub>2</sub>O<sub>3</sub> catalysts where the amount of Na, K, Ca, and Fe are only in their promotor levels.

### 3. Experimental

Scheme 1 shows the lignin hydrotreatment and the workup procedure. The NiMoS/Al<sub>2</sub>O<sub>3</sub> was selected as the representative catalyst, as the kraft lignin contained a significant amount of sulfur impurity from the kraft process; hence, it can avoid the use of an additional sulfiding agent during the hydrotreatment, and the NiMoS is well-known industrially as a cost-effective and sulfur tolerant hydrotreatment catalyst [23,24,29]. The catalyst was synthesized by the incipient wetness impregnation method (Supplementary Materials, Catalyst synthesis S2) The elemental analysis showed 3.85 wt% of Ni and 11.1 wt% of Mo on the Al<sub>2</sub>O<sub>3</sub> support. The catalyst was sulfided before the hydrotreatment using dimethyl disulfide (CH<sub>3</sub>SSCH<sub>3</sub>) (Supplementary Materials, Catalytic lignin depolymerization S5).



**Scheme 1.** Lignin hydrotreatment and workup procedure.

The hydrotreatment was carried out in hexadecane (C<sub>16</sub>H<sub>34</sub>) solvent at a set standard experimental condition of 345 °C, 45 bar of H<sub>2</sub> for 8 h (Supplementary Materials, Catalytic lignin depolymerization S5) The main challenge with a long-chain hydrocarbon solvent when using a NiMoS/Al<sub>2</sub>O<sub>3</sub> catalyst is to minimize the solid residue formation (a repolymerized form of lignin/char that was not converted to liquid products, and the residual lignin) [29]. In general, the amount of solid residue could be reduced or avoided by using oxygen-containing solvents (alcohols acting as capping agents) [18] and hydrogen donor solvents [29]. It is highly desirable to have a solvent without any oxygen moieties for the deoxygenation reaction itself since the solvent otherwise could consume hydrogen. For instance, when dodecane was used as the solvent, Joffres et al. [29] found almost 45 wt% of solid residue formation. In comparison, it was reduced to <8 wt% when tetralin was used as the solvent. In this study, we decided to perform our experiments solely in hexadecane solvent as it gave better separation from oxygenates in our product analysis. Moreover, like dodecane, it could also be sustainably produced by the deoxygenation of vegetable oils [42–44], and intermediate hydrocarbon products like vacuum gas oils are readily available in existing fuel refining processes [45,46].



The reaction products after the hydrotreatment were subjected to filtration to separate the liquid products from the solids (catalyst + solid residue). The liquid product mixtures of the hydrotreatment experiments were analyzed via a GC × GC MS instrument (Supplementary Materials, Product analysis S7). A typical chromatogram is shown in Figure 1A. The chromatogram has five distinctive regions representing cycloalkanes, aromatics, oxygenates, polycyclic hydrocarbons, and polyaromatics. For discussing the deoxygenation activity of the catalysts, mainly the yields of monomeric cycloalkanes, aromatics, and oxygenates (oxygenates undergo deoxygenation to aromatics and cycloalkanes; Figure S1 provides the tentative lignin depolymerization pathway to aromatics and cycloalkanes) were considered. The solids after the filtration were washed with anhydrous acetone to remove the residual hexadecane. The solids were then dried. Subtracting the catalyst's weight from the total weight of solids provides the weight of solid residue generated after the hydrotreatment (Supplementary Materials, Catalytic lignin depolymerization S5 and product analysis S7).

The liquid product after the depolymerization also contains GC × GC undetectable components in the form of higher molecular weight oligomeric products that can be soluble lignin fragments or repolymerization products [29]. Likewise, the solid residue can be a mixture of unconverted lignin, lignin fragments, condensation/repolymerization products that may be char-like compounds, and the inorganic impurities [29].

#### 4. Conclusions

In this study, the role of inorganic impurities of kraft lignin on the deoxygenation activity of a NiMoS/Al<sub>2</sub>O<sub>3</sub> catalyst and on the depolymerization itself was investigated. At first, it was established through recycle runs that during depolymerization, the impurities of kraft lignin were deposited on the catalyst, changing its composition. The recycled catalyst after its thermal regeneration gave a better product yield than the fresh catalyst, indicating that the impurities had a positive role during the catalysis. Conditional experiments with individual impurity elements (i.e., Na, K, Ca, and Fe) confirmed that, at their lower loading, they acted as promoters, but at their higher loading, their poisoning effect was dominant. Since the recycled catalyst had undergone thermal regeneration at the same calcination temperature of the conditional catalysts, the observations of conditional experiments could, to a large extent, be translated to the recycled catalyst's performance. Regardless of their amount, the impurity elements increased the solid residue formation rate. Comparative studies with catalysts containing an equal number of moles of Na and K have shown that the latter is stronger than the former in deactivating the catalyst. However, the synergistic effects of the impurity elements in deactivating the catalyst when present at higher amounts was much stronger and was the crucial factor determining the stability of the catalyst in multiple runs or time-on-stream. <sup>23</sup>Na MAS NMR analysis showed that the Na in kraft lignin existed in a single-site cationic form and as residual Na<sub>2</sub>S. To increase the catalyst life, kraft lignin was subjected to a dilute acetic acid washing pretreatment to remove a large amount of Na and other impurities. The pretreatment showed high efficiency in removing the impurities to insignificant levels. The product yield obtained with the pretreated lignin was higher than the untreated lignin, revealing different roles of impurities when present in the lignin and deposited on the catalyst. During depolymerization, their negative effect dominated the catalytic effect. However, a promoted catalyst can overcome the effect of the impurities on the depolymerization leading to an improved product yield. Nevertheless, the lignin pretreatment is likely the better method to improve both catalyst life and product yield.

**Supplementary Materials:** The following are available online at <https://www.mdpi.com/article/10.3390/catal11080874/s1>, S1: Materials; S2: Catalyst synthesis; S3: Catalyst characterization; S4: Lignin and solid residue characterization; S5: Catalytic lignin depolymerization; S6: Recycle experiments; S7: Product analysis; S8: Pretreatment of kraft lignin; Table S1: Response factors of calibration compounds, Table S2: Complete elemental analysis of kraft lignin; Table S3: Complete elemental analysis of pretreated kraft lignin; Figure S1: Tentative reaction pathway of lignin depolymerization.

Figure S2: TGA/DSC analysis of kraft lignin; Figure S3: Products identification of reaction product obtained over NiMoS/Al<sub>2</sub>O<sub>3</sub>; Figure S4: Chromatogram of the reaction product obtained after the 3rd run of catalyst; Figure S5: Chromatogram of the reaction product obtained over 2.5wt%Na-NiMoS/Al<sub>2</sub>O<sub>3</sub>; Figure S6: <sup>1</sup>H NMR spectra of the kraft lignin and pretreated kraft lignin in DMSO-d<sub>6</sub>; Figure S7: 2D HSQC NMR spectra of (A) and (B) kraft lignin, and (C) and (D) pretreated kraft lignin.

**Author Contributions:** Conceptualization, J.S., D.C., and L.O.; Data curation, J.S., Y.W.C., and D.B.; Methodology, J.S., D.C., and L.O.; Supervision, D.C. and L.O.; Writing—original draft, J.S.; Writing—review and editing, D.B., D.C., and L.O. All authors have read and agreed to the published version of the manuscript.

**Funding:** This work was funded by the Swedish Energy Agency (P47511-1).

**Acknowledgments:** We would like to thank the Swedish Energy Agency for the funding. We would like to acknowledge the Chalmers Material Characterization (CMAL) facilities for microscopy measurements and the NMR center at Gothenburg University for NMR access.

**Conflicts of Interest:** The authors declare no conflict of interest.

## References

1. Zhu, P.; Abdelaziz, O.Y.; Hulteberg, C.P.; Riisager, A. New synthetic approaches to biofuels from lignocellulosic biomass. *Curr. Opin. Green Sustain. Chem.* **2020**, *21*, 16–21. [[CrossRef](#)]
2. Walch, F.; Abdelaziz, O.Y.; Meier, S.; Bjelić, S.; Hulteberg, C.P.; Riisager, A. Oxidative depolymerization of Kraft lignin to high-value aromatics using a homogeneous vanadium–copper catalyst. *Catal. Sci. Technol.* **2021**, *11*, 1843–1853. [[CrossRef](#)]
3. Rinaldi, R.; Jastrzebski, R.; Clough, M.T.; Ralph, J.; Kennema, M.; Bruijninx, P.C.A.; Weckhuysen, B.M. Paving the Way for Lignin Valorisation: Recent Advances in Bioengineering, Biorefining and Catalysis. *Angew. Chem. Int. Ed.* **2016**, *55*, 8164–8215. [[CrossRef](#)] [[PubMed](#)]
4. Li, Y.; Shuai, L.; Kim, H.; Motagamwala, A.H.; Mobley, J.K.; Yue, F.; Tobimatsu, Y.; Havkin-Frenkel, D.; Chen, F.; Dixon, R.A.; et al. An “ideal lignin” facilitates full biomass utilization. *Sci. Adv.* **2018**, *4*, 1–10. [[CrossRef](#)] [[PubMed](#)]
5. Walker, T.W.; Motagamwala, A.H.; Dumesic, J.A.; Huber, G.W. Fundamental catalytic challenges to design improved biomass conversion technologies. *J. Catal.* **2019**, *369*, 518–525. [[CrossRef](#)]
6. McClelland, D.J.; Galebach, P.H.; Motagamwala, A.H.; Wittrig, A.M.; Karlen, S.D.; Buchanan, J.S.; Dumesic, J.A.; Huber, G.W. Supercritical methanol depolymerization and hydrodeoxygenation of lignin and biomass over reduced copper porous metal oxides. *Green Chem.* **2019**, *21*, 2988–3005. [[CrossRef](#)]
7. Abu-Omar, M.M.; Barta, K.; Beckham, G.T.; Luterbacher, J.S.; Ralph, J.; Rinaldi, R.; Román-Leshkov, Y.; Samec, J.S.M.; Sels, B.F.; Wang, F. Guidelines for performing lignin-first biorefining. *Energy Environ. Sci.* **2021**, *14*, 262–292. [[CrossRef](#)]
8. Dessbesell, L.; Paleologou, M.; Leitch, M.; Pulkki, R.; Xu, C. Global lignin supply overview and kraft lignin potential as an alternative for petroleum-based polymers. *Renew. Sustain. Energy Rev.* **2020**, *123*, 109768. [[CrossRef](#)]
9. Chen, H. 3-Lignocellulose biorefinery feedstock engineering. In *Lignocellulose Biorefinery Engineering*; Chen, H., Ed.; Woodhead Publishing: Cambridge, UK, 2015; pp. 37–86.
10. Bruijninx, P.; Weckhuysen, B.; Gruter, G.-J.; Engelen-Smeets, E. *Lignin Valorisation: The Importance of a Full Value Chain Approach*; Utrecht University: Utrecht, The Netherlands, 2016.
11. Dessbesell, L.; Yuan, Z.; Leitch, M.; Paleologou, M.; Pulkki, R.; Xu, C.C. Capacity design of a kraft lignin biorefinery for production of biophenol via a proprietary low-temperature/low-pressure lignin depolymerization process. *ACS Sustain. Chem. Eng.* **2018**, *6*, 9293–9303. [[CrossRef](#)]
12. Demuner, I.F.; Colodette, J.L.; Demuner, A.J.; Jardim, C.M. Biorefinery review: Wide-reaching products through kraft lignin. *BioResources* **2019**, *14*, 7543–7581. [[CrossRef](#)]
13. Lamb, A.C.; Lee, A.F.; Wilson, K. Recent Advances in Heterogeneous Catalyst Design for Biorefining. *Aust. J. Chem.* **2020**, *73*, 832–852. [[CrossRef](#)]
14. Sun, Z.; Fridrich, B.; de Santi, A.; Elangovan, S.; Barta, K. Bright Side of Lignin Depolymerization: Toward New Platform Chemicals. *Chem. Rev.* **2018**, *118*, 614–678. [[CrossRef](#)] [[PubMed](#)]
15. Chowdari, R.K.; Agarwal, S.; Heeres, H.J. Hydrotreatment of Kraft Lignin to Alkylphenolics and Aromatics Using Ni, Mo, and W Phosphides Supported on Activated Carbon. *ACS Sustain. Chem. Eng.* **2019**, *7*, 2044–2055. [[CrossRef](#)] [[PubMed](#)]
16. Horáček, J.; Homola, F.; Kubičková, I.; Kubička, D. Lignin to liquids over sulfided catalysts. *Catal. Today* **2012**, *179*, 191–198. [[CrossRef](#)]
17. Kong, L.; Zhang, L.; Gu, J.; Gou, L.; Xie, L.; Wang, Y.; Dai, L. Catalytic hydrotreatment of kraft lignin into aromatic alcohols over nickel-rhenium supported on niobium oxide catalyst. *Bioresour. Technol.* **2020**, *299*, 122582. [[CrossRef](#)] [[PubMed](#)]
18. Narani, A.; Chowdari, R.K.; Cannilla, C.; Bonura, G.; Frusteri, F.; Heeres, H.J.; Barta, K. Efficient catalytic hydrotreatment of Kraft lignin to alkylphenolics using supported NiW and NiMo catalysts in supercritical methanol. *Green Chem.* **2015**, *17*, 5046–5057. [[CrossRef](#)]

19. Dou, X.; Jiang, X.; Li, W.; Zhu, C.; Liu, Q.; Lu, Q.; Zheng, X.; Chang, H.-m.; Jameel, H. Highly efficient conversion of Kraft lignin into liquid fuels with a Co-Zn-beta zeolite catalyst. *Appl. Catal. B Environ.* **2020**, *268*, 118429. [[CrossRef](#)]
20. Chen, M.; Lu, H.; Wang, Y.; Tang, Z.; Zhang, J.; Wang, C.; Yang, Z.; Wang, J.; Zhang, H. Effect of Reduction Treatments of Mo/Sepiolite Catalyst on Lignin Depolymerization under Supercritical Ethanol. *Energy Fuels* **2020**, *34*, 3394–3405. [[CrossRef](#)]
21. Mortensen, P.M.; Grunwaldt, J.D.; Jensen, P.A.; Knudsen, K.G.; Jensen, A.D. A review of catalytic upgrading of bio-oil to engine fuels. *Appl. Catal. A Gen.* **2011**, *407*, 1–19. [[CrossRef](#)]
22. Elliott, D.C.; Peterson, K.L.; Muzatko, D.S.; Alderson, E.V.; Hart, T.R.; Neuenschwander, G.G. Effects of trace contaminants on catalytic processing of biomass-derived feedstocks. *Appl. Biochem. Biotechnol.* **2004**, *115*, 807–825. [[CrossRef](#)]
23. Stummann, M.Z.; Høj, M.; Hansen, A.B.; Beato, P.; Wiwel, P.; Gabrielsen, J.; Jensen, P.A.; Jensen, A.D. Deactivation of a CoMo Catalyst during Catalytic Hydropyrolysis of Biomass. Part 1. Product Distribution and Composition. *Energy Fuels* **2019**, *33*, 12374–12386. [[CrossRef](#)]
24. Stummann, M.Z.; Høj, M.; Davidsen, B.; Hansen, L.P.; Beato, P.; Gabrielsen, J.; Jensen, P.A.; Jensen, A.D. Deactivation of a CoMo Catalyst during Catalytic Hydropyrolysis of Biomass. Part 2. Characterization of the Spent Catalysts and Char. *Energy Fuels* **2019**, *33*, 12387–12402. [[CrossRef](#)]
25. Tribot, A.; Amer, G.; Abdou Alio, M.; de Baynast, H.; Delattre, C.; Pons, A.; Mathias, J.-D.; Callois, J.-M.; Vial, C.; Michaud, P.; et al. Wood-lignin: Supply, extraction processes and use as bio-based material. *Eur. Polym. J.* **2019**, *112*, 228–240. [[CrossRef](#)]
26. Bermudez, J.M.; Fidalgo, B. 15-Production of bio-syngas and bio-hydrogen via gasification. In *Handbook of Biofuels Production*, 2nd ed.; Luque, R., Lin, C.S.K., Wilson, K., Clark, J., Eds.; Woodhead Publishing: Duxford, UK, 2016; pp. 431–494.
27. Patton, R.; Steele, P.; Yu, F. Coal vs. Charcoal-fueled Diesel Engines: A Review. *Energy Sources Part A Recovery Util. Environ. Eff.* **2009**, *32*, 315–322. [[CrossRef](#)]
28. Munick de Albuquerque Frago, D.; Bouxin, F.P.; Montgomery, J.R.D.; Westwood, N.J.; Jackson, S.D. Catalytic depolymerisation of isolated lignin to fine chemicals: Depolymerisation of Kraft lignin. *Bioresour. Technol. Rep.* **2020**, *9*, 100400. [[CrossRef](#)]
29. Joffres, B.; Nguyen, M.T.; Laurenti, D.; Lorentz, C.; Souchon, V.; Charon, N.; Daudin, A.; Quignard, A.; Geantet, C. Lignin hydroconversion on MoS<sub>2</sub>-based supported catalyst: Comprehensive analysis of products and reaction scheme. *Appl. Catal. B Environ.* **2016**, *184*, 153–162. [[CrossRef](#)]
30. Nakadi, F.V.; Prodanov, C.; Boschetti, W.; Vale, M.G.R.; Welz, B.; de Andrade, J.B. Determination of silicon in biomass and products of pyrolysis process via high-resolution continuum source atomic absorption spectrometry. *Talanta* **2018**, *179*, 828–835. [[CrossRef](#)]
31. Wu, J.-W.; Shi, Y.; Zhu, Y.-X.; Wang, Y.-C.; Gong, H.-J. Mechanisms of Enhanced Heavy Metal Tolerance in Plants by Silicon: A Review. *Pedosphere* **2013**, *23*, 815–825. [[CrossRef](#)]
32. Molino, A.; Chianese, S.; Musmarra, D. Biomass gasification technology: The state of the art overview. *J. Energy Chem.* **2016**, *25*, 10–25. [[CrossRef](#)]
33. Zhang, L.; Tang, S.; Guan, Y. Excellent Adsorption–Desorption of Ammonium by a Poly(acrylic acid)-Grafted Chitosan and Biochar Composite for Sustainable Agricultural Development. *ACS Sustain. Chem. Eng.* **2020**, *8*, 16451–16462. [[CrossRef](#)]
34. Gupta, S.; Mondal, P.; Borugadda, V.B.; Dalai, A.K. Advances in upgradation of pyrolysis bio-oil and biochar towards improvement in bio-refinery economics: A comprehensive review. *Environ. Technol. Innov.* **2021**, *21*, 101276. [[CrossRef](#)]
35. Surisetty, V.R.; Tavasoli, A.; Dalai, A.K. Synthesis of higher alcohols from syngas over alkali promoted MoS<sub>2</sub> catalysts supported on multi-walled carbon nanotubes. *Appl. Catal. A Gen.* **2009**, *365*, 243–251. [[CrossRef](#)]
36. Brauckmann, J.O.; Verhoef, R.; Schotman, A.H.M.; Kentgens, A.P.M. Solid-State Nuclear Magnetic Resonance Characterization of Residual <sup>23</sup>Na in Aramid Fibers. *J. Phys. Chem. C* **2019**, *123*, 14439–14448. [[CrossRef](#)]
37. Verhulst, H.A.M.; Welters, W.; Vorbeck, G.; Ljm, V.; Vhj, B.; van Santen, R.; Haan, J. A new assignment of the signals in <sup>23</sup>Na DOR NMR to sodium sites in dehydrated Na Y Zeolite. *J. Phys. Chem.* **1994**, *98*, 639–7062. [[CrossRef](#)]
38. O’Connell, E.M.; Root, T.W.; Cooper, S.L. Morphological studies of lightly-sulfonated polystyrene using <sup>23</sup>Na NMR. 1. Effects of sample composition. *Macromolecules* **1994**, *27*, 5803–5810. [[CrossRef](#)]
39. Persson, H.; Kantarelis, E.; Evangelopoulos, P.; Yang, W. Wood-derived acid leaching of biomass for enhanced production of sugars and sugar derivatives during pyrolysis: Influence of acidity and treatment time. *J. Anal. Appl. Pyrolysis* **2017**, *127*, 329–334. [[CrossRef](#)]
40. Klett, A.S.; Payne, A.M.; Thies, M.C. Continuous-Flow Process for the Purification and Fractionation of Alkali and Organosolv Lignins. *ACS Sustain. Chem. Eng.* **2016**, *4*, 6689–6694. [[CrossRef](#)]
41. Pinheiro Pires, A.P.; Arauzo, J.; Fonts, I.; Domine, M.E.; Fernández Arroyo, A.; Garcia-Perez, M.E.; Montoya, J.; Chejne, F.; Pfromm, P.; Garcia-Perez, M. Challenges and Opportunities for Bio-oil Refining: A Review. *Energy Fuels* **2019**, *33*, 4683–4720. [[CrossRef](#)]
42. Yoosuk, B.; Sanggam, P.; Wiengket, S.; Prasassarakich, P. Hydrodeoxygenation of oleic acid and palmitic acid to hydrocarbon-like biofuel over unsupported Ni-Mo and Co-Mo sulfide catalysts. *Renew. Energy* **2019**, *139*, 1391–1399. [[CrossRef](#)]
43. Baharudin, K.B.; Taufiq-Yap, Y.H.; Hunns, J.; Isaacs, M.; Wilson, K.; Derawi, D. Mesoporous NiO/Al-SBA-15 catalysts for solvent-free deoxygenation of palm fatty acid distillate. *Microporous Mesoporous Mater.* **2019**, *276*, 13–22. [[CrossRef](#)]
44. Arora, P.; Abdolahi, H.; Cheah, Y.W.; Salam, M.A.; Grennfelt, E.L.; Rådberg, H.; Creaser, D.; Olsson, L. The role of catalyst poisons during hydrodeoxygenation of renewable oils. *Catal. Today* **2021**, *367*, 28–42. [[CrossRef](#)]

- 
45. Badoga, S.; Alvarez-Majmutov, A.; Xing, T.; Gieleciak, R.; Chen, J. Co-processing of Hydrothermal Liquefaction Biocrude with Vacuum Gas Oil through Hydrotreating and Hydrocracking to Produce Low-Carbon Fuels. *Energy Fuels* **2020**, *34*, 7160–7169. [[CrossRef](#)]
  46. Ivanova, A.S.; Korneeva, E.V.; Bukhtiyarova, G.A.; Nuzhdin, A.L.; Budneva, A.A.; Prosvirin, I.P.; Zaikovskii, V.I.; Noskov, A.S. Hydrocracking of vacuum gas oil in the presence of supported nickel-tungsten catalysts. *Kinet. Catal.* **2011**, *52*, 446–458. [[CrossRef](#)]